

A single arrangement variational method for reactive scattering: Total and state-resolved reaction probabilities

Xudong Wu^{a)}

Department of Chemistry and Biochemistry, University of Texas, Austin, Texas 78712

B. Ramachandran

Department of Chemistry, Louisiana Tech University, Ruston, Louisiana 71272

Robert E. Wyatt

Department of Chemistry and Biochemistry, University of Texas, Austin, Texas 78712

(Received 11 July 1994; accepted 16 August 1994)

A detailed discussion of an approximate, variational approach to atom-molecule reactive scattering is presented. This approach reduces the formally three arrangement atom-diatomic molecule reactive scattering problem to one of a single arrangement without the use of negative imaginary potentials at the exit channel boundaries. The method is based on applying the Kohn variational principle for the log-derivative matrix to a representation of the scattering wave function that spans just the reactant arrangement. For many reactive systems, the method yields impressively accurate results for total reaction probabilities from a specific initial state. In such cases, it is also possible to extract fairly accurate state-resolved reaction probabilities from the results of the variational calculation. The mathematical and practical aspects of accomplishing this are presented. We evaluate the advantages and the limitations of the method by numerical computations on the collinear $H+H_2$ (and isotopes) and $F+H_2$, and the three dimensional ($J=0$) $F+H_2$ reactions. © 1994 American Institute of Physics.

I. INTRODUCTION

In a recent letter,¹ we outlined an approximate method for the computation of total reaction probabilities from a specific initial state in the case of atom-diatomic molecule reactive scattering. This method yields an approximate scattering matrix from a variational calculation of the log-derivative matrix, where the trial function is a representation of the scattering wave function spanning only the reactant arrangement. Preliminary results¹ indicated that the method had sufficient potential to warrant further investigation. This paper presents a more complete discussion of this method, as well as an extension to the method that enables one to calculate state-resolved reaction probabilities from the results of the variational calculation.

The development of methods that reduce the computational effort involved in a formally exact treatment of the three-body reactive scattering problem has attracted considerable attention in the recent past.²⁻⁷ The general trend in this area has been to seek a reduction in the size of the domain spanned by the solutions, i.e., the scattering wave functions. To this end, Neuhauser, Baer, and co-workers use negative imaginary potentials (NIPs) at the boundaries of the entrance and exit channels,²⁻⁴ while Miller and co-workers place these potentials on the borders of the "transition state region."⁵⁻⁷ Both approaches result in substantial reductions in the size of the regions that must be spanned by basis functions, thus reducing the computational effort involved in these calculations. A different approach was taken by Mandelshtam and Taylor,⁸ who compute cumulative reaction

probabilities by enclosing the interaction region of the potential in successively larger "boxes" with infinite potentials at the boundaries.

The method developed by us¹ also reduces the size of the coordinate space spanned by the basis functions. The method does this by reducing the three-arrangement scattering problem to a two-point boundary value problem in a single arrangement. However, it accomplishes this without the use of the NIPs and thereby avoids the complications, the increased computational effort, and storage requirements resulting from complex algebra. The fact that such a boundary value problem can be solved by a suitable variational method⁹⁻¹¹ adds to the attractiveness of the present method.

The main features of the present method are the following: The scattering problem is solved in a small region spanned by the mass-weighted Jacobi vectors (\mathbf{R}, \mathbf{r}) for the reactant arrangement. Schematically, for the sake of this discussion, we represent this region as a rectangle, as shown in Fig. 1. The Kohn variational principle for the log-derivative matrix⁹⁻¹¹ is used to compute the log-derivative matrix at the boundaries $R=R_N$ and $r=r_M$, with the gradients computed perpendicular to the boundaries, i.e., with respect to R at $R=R_N$ and with respect to r at $r=r_M$. From this approximate log-derivative matrix, an approximate scattering matrix is constructed by applying complex incoming and outgoing wave boundary conditions at $R=R_N$ and $r=r_M$, perpendicular to the boundaries. This last step also requires the evaluation of a set of bound-state energy eigenvalues at the boundaries so that the wave vectors for the complex waves can be evaluated.

This approach is, of course, necessarily approximate. The scattering boundary conditions applied above will be exact only if the mass-weighted angles between the reactant

^{a)}Present address: Department of Chemistry, Ohio State University, Columbus, OH 43210.

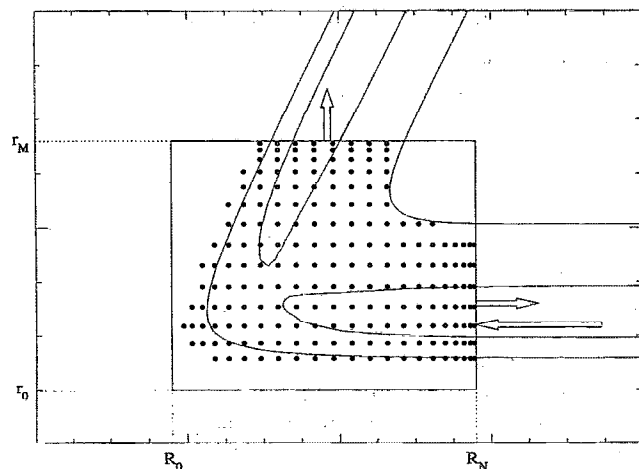


FIG. 1. A schematic summary of the single arrangement method: the scattering problem is solved in the rectangular region, and the S -matrix boundary conditions are applied at $R=R_N$ and $r=r_M$. Two contours of the potential surface and the DVR points selected by applying the energy cut-off criteria (see the text) are shown. All distances are in atomic units (bohrs).

and product arrangements were exactly 90° , which occurs only in the case of molecule-surface scattering. As the angles become smaller, the boundary conditions applied at the product boundary $r=r_M$ become poorer approximations to the correct boundary conditions. In spite of this, however, previous applications of the method¹ to reactive systems in which the mass-weighted angles were as sharp as 54.7° showed that the total reaction probabilities from a specific initial state computed using these approximate boundary conditions were surprisingly accurate over a wide range of energies. In the present paper, we show that the method succeeds even in cases where the angle is as small as 41.4° . Moreover, as we show below, when the total reaction probabilities from the present approach are accurate, the variational solutions are sufficiently close to the actual solutions that we can extract fairly accurate state-to-state resolved reaction probabilities from them.

At the same time, we find that this approach does not work equally well in all cases. One of the examples we present below is one where the method does not yield accurate results for a certain range of scattering energies. Examining the reasons for the failure in this case leads to interesting insights and suggests ways to further improve the method.

It should be noted that well-known procedures exist to make the results from our approximate method exact. These are the various techniques for log-derivative matrix propagation¹²⁻¹⁴ or R -matrix propagation.¹⁵ Once the solutions at the boundaries of the rectangular region are calculated using the method described below, any of the above-mentioned propagation schemes can, in principle, yield the exact result.

The remainder of this paper is organized as follows: In Sec. II, we present the mathematical details of formulating the variational problem in a single arrangement and the considerations to be used in the selection of basis functions for

representing the solutions. Section III presents the numerical tests conducted to evaluate the method. The majority of these tests are done using collinear models and compute the total reaction probabilities from a specific initial state. However, one three-dimensional application is presented here (in addition to those in Ref. 1) in order to support some of our conclusions. In Sec. IV, we show how state-to-state probabilities can be extracted from the solutions of the variational calculation. Section V summarizes our investigations and presents an evaluation of the advantages and limitations of the present method.

II. MATHEMATICAL AND COMPUTATIONAL ASPECTS

The mathematical foundation for our method is provided by the Kohn variational principle for the log-derivative matrix, or the Y matrix (Y -KVP).⁹⁻¹¹ A detailed discussion of this variational principle appears in Ref. 10. However, the following details, along with Fig. 1, should be sufficient for understanding this approach to reactive scattering. In order to keep our equations reasonably free of clutter, we use the collinear reactive scattering case to present the formulation of the Y -KVP in a single arrangement. Extending this formulation to the three-dimensional case requires a few additional details, which we will discuss subsequently.

A. Formulation for collinear reactive scattering

The variational functional for the log-derivative Y may be written as

$$Y = Y_0 + \langle \Psi | H - E | \Psi \rangle, \quad (1)$$

where Y_0 is a "guess" for the stationary quantity (see Ref. 10). For collinear scattering, the functions $\Psi^m(R, r)$, where the superscript indicates the initial state, satisfy the equation

$$-\frac{\hbar^2}{2\mu} \left(\frac{\partial^2 \Psi^m}{\partial R^2} + \frac{\partial^2 \Psi^m}{\partial r^2} \right) + V(R, r) \Psi^m = E \Psi^m, \quad (2)$$

where the coordinates are mass-weighted Jacobi coordinates for the reactant arrangement.¹⁶ The stationary expression for the (m, n) element of the log-derivative matrix at the boundaries $r=r_M$ ($R_0 \leq R \leq R_N$); $R=R_N$ ($r_0 \leq r \leq r_M$) is now obtained as⁹⁻¹¹

$$Y_{mn} = \int_{R_0}^{R_N} dR \int_{r_0}^{r_M} dr \left[\left(\frac{\partial \Psi^m}{\partial R} \right) \left(\frac{\partial \Psi^n}{\partial R} \right) + \left(\frac{\partial \Psi^m}{\partial r} \right) \times \left(\frac{\partial \Psi^n}{\partial r} \right) \right] + \frac{2\mu}{\hbar^2} \int_{R_0}^{R_N} dR \int_{r_0}^{r_M} dr \Psi^m \times [V(R, r) - E] \Psi^n. \quad (3)$$

The solution corresponding to a reactant initial state m is required to satisfy the conditions $\Psi^m(R_N, r) = \phi_m(r)$ at $R=R_N$, where $\phi_m(r)$ are solutions to the bound state problem

$$-\frac{\hbar^2}{2\mu} \frac{\partial^2 \phi_m}{\partial r^2} + V(R_N, r) \phi_m(r) = \epsilon_m \phi_m(r); \quad m=0, 1, 2, \dots \quad (4a)$$

and $\Psi^m(R, r_M) = 0$, whereas a solution corresponding to a "product" initial state n is required to satisfy the condition $\Psi^n(R, r_M) = \varphi_n(R)$ at $r = r_M$, where $\varphi_n(R)$'s are solutions to

$$-\frac{\hbar^2}{2\mu} \frac{\partial^2 \varphi_n}{\partial R^2} + V(R, r_M) \varphi_n(R) = \epsilon'_n \varphi_n(R), \quad n=0, 1, 2, \dots \quad (4b)$$

and $\Psi^n(R_N, r) = 0$. Thus, the solutions satisfying the "log-derivative boundary conditions" become identical to the initial diatomic wave functions at the appropriate boundary and vanish at all the other boundaries of the problem. Once the log-derivative matrix is found, the S matrix boundary conditions¹⁰ are applied at $R = R_N$ and $r = r_M$ using the internal energies calculated from Eqs. (4), and the total reaction probability from a specific initial state is obtained by summing the appropriate column of the reactive block of $|S|^2$.

The approximate nature of our approach arises from the fact that the derivative of the wave function at the $r = r_M$ boundary is evaluated in a direction perpendicular to the reactant translational coordinate. Moreover, the bound state problem of Eq. (4b) involves a potential for internal motion that does not correspond to the product diatomic internal motion. In spite of these unphysical features, the total reaction probabilities calculated using the method are accurate over a wide range of energies for certain reactions, as shown in the following section. It will be seen there that even in cases where we would expect this approach to fail completely, the results are qualitatively and often quantitatively quite close to the exact results. It should be noted, however, that the individual elements of the S matrix obtained in this fashion are most often not close to those of the actual S matrix.

We now turn to the computational details of obtaining the Y matrix using the Kohn variational principle. We expand $\Psi^m(R, r)$ in the region ($R_0 \leq R \leq R_N$; $r_0 \leq r \leq r_M$) as

$$\Psi^m(R, r) = \sum_{i=1}^N \sum_{j=1}^M |u_i(R) v_j(r)\rangle \langle u_i(R) v_j(r) | \Psi^m, \quad (5)$$

where $u_i(R)$ and $v_j(r)$ are L^2 basis functions which satisfy the log-derivative boundary conditions⁹⁻¹¹

$$u_i(0) = u_i(R_N) = 0, \quad i = 1, \dots, N-1, \quad (6a)$$

$$u_N(0) = 0, \quad u_N(R_N) = 1. \quad (6b)$$

$$v_j(0) = v_j(r_M) = 0, \quad j = 1, \dots, M-1, \quad (6c)$$

$$v_M(0) = 0, \quad v_M(r_M) = 1. \quad (6d)$$

The substitution of Eq. (5) into Eq. (3) followed by the extremization of the functional with respect to the (as yet unknown) expansion coefficients $C_{ij}^m = \langle u_i v_j | \Psi^m \rangle$ results in a linear algebraic system of equations with multiple right-hand sides $\mathbf{AC} = \mathbf{B}$, which must be solved for the coefficients \mathbf{C} . The matrix elements of \mathbf{A} and \mathbf{B} are given as

$$\begin{aligned} A_{ijkl} = & \langle u'_i | u'_k \rangle \langle v_j | v_l \rangle + \langle v'_j | v'_l \rangle \langle u_i | u_k \rangle \\ & + \frac{2\mu}{\hbar^2} \langle u_i v_j | V - E | u_k v_l \rangle, \end{aligned} \quad (7a)$$

$$\begin{aligned} B_{ij}^m = & \langle u'_i | u'_N \rangle \langle v_j | \phi_m \rangle + \langle v'_j | \phi'_m \rangle \langle u_i | u_N \rangle \\ & + \frac{2\mu}{\hbar^2} \langle u_i v_j | V - (E' - \epsilon_m) | u_N \phi_m \rangle \end{aligned} \quad (7b)$$

where we have used the fact that $\Psi^m(R_N, r) = u_N \phi_m(r)$ in evaluating the block \mathbf{B}^m . A similar set of matrix elements also exists for "product" initial states, and these make up the \mathbf{B}^n block of the right-hand sides. The only differences between \mathbf{B}^m and \mathbf{B}^n are that in the latter, the internal functions are functions of R , and we use the fact $\Psi^n(R, r_M) = v_M \varphi_n(R)$ in order to define the right-hand sides.

The basis functions $\{u_i\}$ and $\{v_j\}$ are chosen, respectively, to be Lagrange polynomials defined over $(N+1)$ -point and $(M+1)$ -point¹⁷ Gauss-Lobatto quadrature nodes. This automatically ensures that the boundary conditions of Eqs. (6) are satisfied. In addition, at each quadrature node, these functions satisfy the Kronecker delta conditions $u_i(R_k) = \delta_{ik}$ and $v_j(r_l) = \delta_{jl}$.¹⁸ In other words, this choice of the basis functions and the quadrature rule give rise to a discrete variable representation (DVR)^{9,19} of the problem on a grid in the rectangular region of Fig. 1.

The computational advantages of a DVR are well known and have been discussed in many recent publications.^{1,5-7,9,19} In the present case, the DVR directly helps to determine a few of the expansion coefficients in Eq. (5) from the solutions of the one-dimensional problems of Eqs. (4), since $\phi_m(r_l) = \langle u_N v_l | \Psi^m \rangle$; $l = 1, \dots, M$ and $\varphi_n(R_k) = \langle u_k v_M | \Psi^n \rangle$; $k = 1, \dots, N$. The DVR also causes a large number of matrix elements in \mathbf{A} and \mathbf{B} to vanish, since

$$A_{ijkl} = \langle u'_i | u'_k \rangle \delta_{jl} + \langle v'_j | v'_l \rangle \delta_{ik} + \frac{2\mu}{\hbar^2} [V(R_i, r_j) - E] \delta_{ik} \delta_{jl}, \quad (8a)$$

$$\begin{aligned} B_{ij}^m = & \langle u'_i | u'_N \rangle \delta_{jl} + \langle v'_j | \phi^m \rangle \delta_{iN} + \frac{2\mu}{\hbar^2} [V(R_i, r_j) \\ & - (E - \epsilon_m)] \delta_{iN}. \end{aligned} \quad (8b)$$

Since all the expansion coefficients corresponding to $i = N$ and $j = M$ are known from the boundary conditions, the range of the indices i and k in \mathbf{A} and \mathbf{B}^m extends from $1, \dots, (N-1)$. This means that the only nonzero term in Eq. (8b) is the first term. Similar arguments (for the range of indices j and l) can be offered in the case of the \mathbf{B}^n (or the "product") block of the right-hand side to show that only one of the kinetic energy terms survives in that case also.

It is easy to see that Eqs. (8) give rise to a very sparse matrix \mathbf{A} and a sparse set of right-hand sides \mathbf{B} . It is especially interesting that the Kronecker delta property of the basis functions gives rise to a very structured matrix. The largest matrix elements of matrix \mathbf{A} occur along the diagonal, which are the only terms with a contribution from the potential and the scattering energy. The vast majority of the remaining nonzero elements occur in diagonal blocks. Outside the diagonal blocks, the nonzero matrix elements become successively smaller and occur in "stripes" parallel to the diagonal. Such a matrix is ideally suited for solution by the several iterative methods available today,²⁰⁻²⁴ which do not require the full matrix to be stored in memory. We have

already implemented the generalized minimal residual (GMRes) method²⁰ with a preconditioner²³ to solve the linear algebraic problem, and the preliminary results have been encouraging.²⁵

In the collinear applications presented below, we have opted to solve the relatively small linear system of equations directly. The three-dimensional applications presented in Ref. 1 exploit the structured sparsity of **A** to achieve significant savings in memory, and use an iterative refinement scheme to converge the solutions. The 3D application presented in Sec. III also exploits the structured sparsity of **A** in the same fashion, but utilizes the GMRes algorithm.

B. Extension to three-dimensional reactive scattering

Extending this approach to three-dimensional reactive scattering involves a few more details, which we now discuss. The scattering wave functions $\Psi^m(R, r, \gamma) = (Rr)^{-1} \psi^m(R, r, \gamma)$ in this case satisfy

$$\begin{aligned} &-\frac{\hbar^2}{2\mu} \left(\frac{\partial^2 \psi^m}{\partial R^2} + \frac{\partial^2 \psi^m}{\partial r^2} - \frac{\hat{L}^2}{R^2} \psi^m - \frac{j^2}{r^2} \psi^m \right) + V(R, r, \gamma) \psi^m \\ &= E \psi^m, \end{aligned} \quad (9)$$

where (R, r, γ) are the mass-weighted Jacobi coordinates¹⁶ for the reactant arrangement. These functions are expressed in terms of the Gauss-Lobatto DVR and a set of spherical harmonics as

$$\psi^m(R, r, \gamma) = \sum_{i=1}^N \sum_{k=1}^M \sum_{j=1}^{j_{\max}} |u_i(R) v_k(r) Y_{j,l}^{JM}\rangle \langle u_i v_k Y_{j,l}^{JM} | \psi^m \rangle, \quad (10)$$

where $Y_{j,l}^{JM}$'s are defined as¹⁶

$$Y_{j,l}^{JM} = \sum_{m_j, m_l} \langle j l m_j m_l | j l J M \rangle Y_{j, m_j}(\hat{r}) Y_{l, m_l}(\hat{R}). \quad (11)$$

Since $|j-l| \leq J \leq j+l$, the values of J and j above determine the allowed values of l . The quantity j_{\max} is a parameter chosen based on the diatomic bound-state energies and the scattering energy.

The three-dimensional analogs of the reactant and "product" internal functions defined in Eqs. (4) are obtained as follows: The reactant internal functions satisfy the equation

$$\left\{ \frac{-\hbar^2}{2\mu} \left[\frac{\partial^2}{\partial r^2} - \frac{j(j+1)}{r^2} \right] + V(R_N, r, 0) - \epsilon_{v_j} \right\} \phi_{v_j}(r) = 0, \quad (12a)$$

while the product internal functions are defined as solutions to the equation

$$\begin{aligned} &\left\{ \frac{-\hbar^2}{2\mu} \left[\frac{\partial^2}{\partial R^2} - \frac{l(l+1)}{R^2} \right] \right. \\ &\left. + V_{j l j' l'}(R, r_M) - \epsilon'_{v_j l j' l'} \right\} \chi_{v_j l j' l'} = 0, \end{aligned} \quad (12b)$$

where $V_{j l j' l'}(R, r_M)$ is defined as

$$V_{j l j' l'}(R, r_M) = \langle Y_{j l}^{JM}(\gamma) | V(R, r_M, \gamma) | Y_{j' l'}^{JM}(\gamma) \rangle. \quad (13)$$

TABLE I. The parameters for typical runs for the collinear reactions. Lengths are in bohrs and energies in electron volts.

Parameter	H+H ₂	F+H ₂
R_0	0.0000	0.0000
R_N	6.5000	6.5000
r_0	0.0000	0.0000
r_M	3.5000	3.0000
Scattering energy (range)	0.40–1.65	0.28–0.80
Energy cut-off parameter ^a	2.0000	1.5000
Full basis size $(N-1) \times (M-1)$	1666	1421
Selected basis size N_{sel}	386	397

^aThe energy cutoff used on the repulsive side of the potential is twice the cut-off parameter listed.

It is necessary to define the product internal states with respect to effective potentials generated by averaging over the angle γ at the boundary $r=r_M$ because the potential $V(R, r, \gamma)$ typically has strong dependence on the angle γ at the boundary $r=r_M$. Although this may appear somewhat inelegant, having to evaluate the matrix elements of Eq. (13), or the solutions of Eqs. (12), are not significant difficulties in the applications of the method. First of all, even large eigenvalue-eigenvector problems can be very efficiently solved on modern supercomputers with highly optimized routines. Second, only a few of the bound states at $r=r_M$ have to be converged in order to yield accurate total reaction probabilities. Note that the scattering wave functions in the "interaction region" of the potential are represented by functions (DVR points) independent of the asymptotic diatomic states. Therefore, the log-derivative matrix, in principle, need consist only of matrix elements between the open channels at each scattering energy. This also means that the basis set expansion for the solutions of Eq. (14b) need only be sufficiently large to converge the open channels.

The substitution of the Hamiltonian of Eq. (9), basis set expansion of Eq. (10), and the solutions of Eqs. (12) into the variational functional of Eq. (1), followed by extremization of the functional with respect to the expansion coefficients, results in a linear algebraic system of equations with structured sparsity, as in the case of the collinear model. The order of the matrix **A** in this case will be $(N-1) \times (M-1) \times j_{\max}$. In actual applications, we further reduce the size of the matrices **A** and **B** by rejecting all DVR points that lie in regions where the potential is higher than an arbitrary energy cut-off parameter. The grid points shown in Fig. 1 are the points selected by applying such a cutoff. In the case of collinear scattering, the potential has the same dimensionality as the DVR grid, and a simple scanning of the potential is sufficient to select a physically relevant subset of the grid points. In 3D scattering, in principle, one must scan the angle γ at each grid point (R_i, r_k) to check whether the potential energy falls below the cutoff. In the present set of applications, however, we have applied the cut-off criteria by scanning the potential $V(R, r, \gamma)$ at three values of the angle γ . Applying the cut-off criteria typically results in a 50% or greater reduction in the order of matrix **A**. Tables I and II present typical values for the parameters used in several of the calculations.

TABLE II. The parameters for typical runs for the three-dimensional reactions. Lengths are in bohrs and the energies in electron volts.

Parameter	H+H ₂	F+H ₂
R_0	1.0000	1.0000
R_N	6.0000	6.5000
r_0	0.0000	0.3000
r_M	4.5000	2.3000
Scattering energy (range)	0.28–1.65	0.29–0.50
Energy cut-off parameter ^a	2.0000	1.5000
j_{\max}	30	40
DVR basis size $(N-1) \times (M-1)$	853	897
Selected basis size N_{sel}	365	408

^aThe energy cutoff used on the repulsive side of the potential is twice the cut-off parameter listed.

III. TOTAL REACTION PROBABILITY FROM SPECIFIC INITIAL STATES

In this section, we describe the numerical tests we have conducted in order to evaluate the method, and present the results. While the bulk of the tests are conducted on collinear models, a three-dimensional application is presented here in order to support one of the conclusions regarding the range of applicability of the method. Applications of the method to the 3D H+H₂, D+H₂, and H+D₂ reactions ($J=0$) have already been presented in Ref. 1, and are not repeated here.

We first examine the sensitivity of the total reaction probabilities on the position of the boundary r_M on the product side. Figure 2 shows the total reaction probability from the ground state of the H₂ molecule for the collinear H+H₂ reaction on the *PK2* surface for several values of r_M . We also show the exact results, obtained from a two-arrangement formulation of the *Y-KVP* method, in Fig. 2. Clearly, in this case, the results from the method are reasonably insensitive to the position of the boundary on the product side. Figure 2 also indicates that the results are in good agreement with those of the exact calculation. Similar agreement is found for the total reaction probabilities out of the first and second excited states of the H₂ molecule as well.

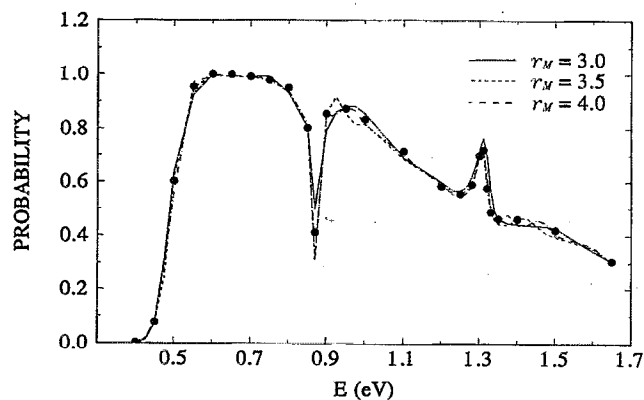


FIG. 2. The total reaction probability from the reactant $\nu=0$ state for the collinear H+H₂ reaction on the *PK2* surface. The results of the single arrangement method at different values of the product boundary r_M are shown as lines, and the exact results are represented by the symbols.

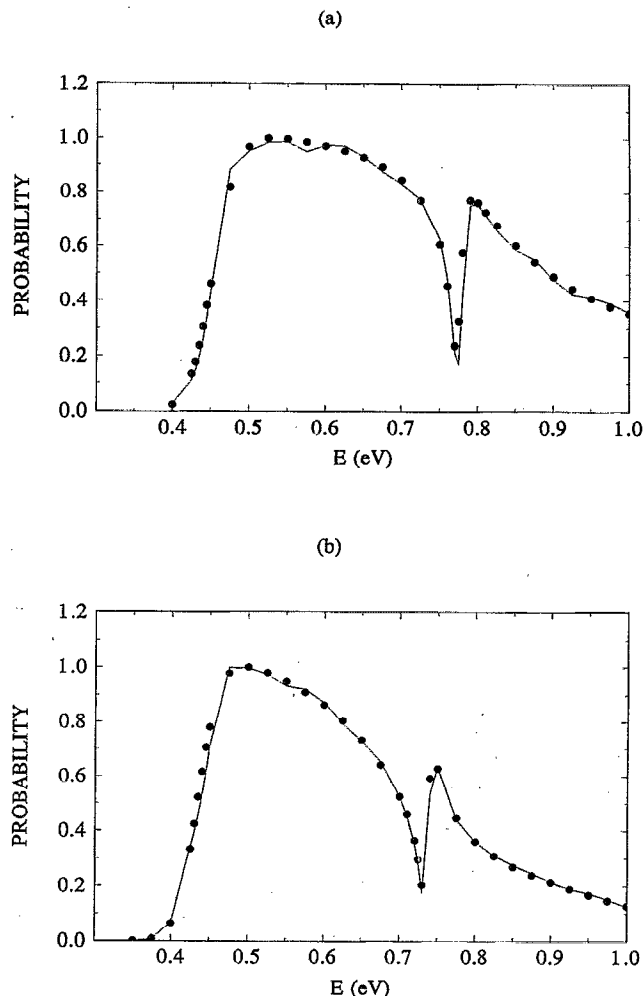


FIG. 3. The total reaction probability from the reactant $\nu=0$ state for two collinear reactions on the *PK2* surface. The results of the single arrangement method are shown as lines, and the exact results are represented by the symbols. (a) The D+HD reaction; (b) the T+HT reaction ($T=^3\text{H}$).

As noted in the Introduction, the boundary conditions applied at the product boundary become worse approximations to the correct boundary conditions as the mass-weighted angle between the two arrangements decreases. We now examine how this affects the results of the single arrangement method by increasing the masses of the nonexchanged atoms. In Fig. 3, we present the total reaction probabilities for the D+HD (mass-weighted angle=48.6°) and the T+HT ($T=^3\text{H}$) reactions (mass-weighted angle=41.4°). Clearly, there is good agreement between the results of the present method and the exact results. Although not shown in Fig. 3, we have repeated these calculations at different values of r_M and verified that the results are stable.

However, the application of the present method to the collinear F+H₂ reaction (mass-weighted angle=46.4°) on the *T5A* surface,²⁶ produces quite different results. As seen in Fig. 4, at low energies, the total reaction probability fluctuates wildly as r_M is varied. In this region, the results of the present method are also in poor agreement, even qualitatively, with the exact ones. However, as the energy increases,

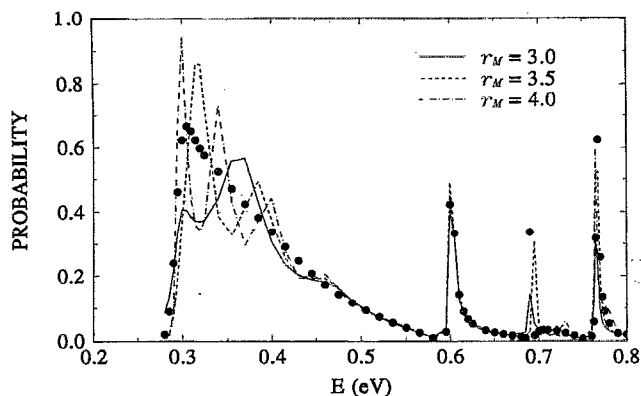


FIG. 4. The same as Fig. 2, but for the $F+H_2$ reaction on the TSA surface.

the sensitivity of the reaction probabilities to r_M decreases dramatically, and the agreement between the single arrangement and the exact results improves considerably.

In light of the results presented in Fig. 3, we may discount the small value of the mass-weighted angle as the source of this behavior. That explanation, in any case, fails to explain why the results are in poor agreement with the exact ones only at energies near the threshold. We believe that the sensitive dependence of the near-threshold reaction probabilities on the position of the product boundary r_M is caused by factors that affect the free flow of reactive flux from the "strong interaction" region to the asymptotic product region. These factors can be identified by the following reasoning:

The behavior of the scattering wave functions in the exit channel away from the product boundary is largely determined by the local potential. It is well known that for this reaction, on the TSA surface, reactive flux into the HF $\nu=3$ vibrational state is energetically favored at energies near the threshold. This means that the exit channel solution will have a significant $\nu=3$ component. The boundary conditions applied at $r=r_M$, however, depend on the bound state energies calculated using the potential $V(R, r_M)$. Table III presents the product bound state energies of HF, calculated both along a cut of the product channel potential at the proper mass-weighted angle (along r' at fixed R' , say $R' = R'_N$; the

following section explains how R'_N is chosen) and along $r=r_M$. Table III shows that the scattering wave function at near-threshold energies ($E \sim 0.28$ eV) in the case of the $F+H_2$ reaction is matched to vibrational states whose energies are significantly different from the vibrational states supported by the exit channel potential away from the boundary. In fact, the shape of the potential in the single arrangement approach, which is implied by the boundary conditions applied, is similar to that shown in Fig. 5(a). In dynamical terms, it is as if the potential suddenly and discontinuously widens (the "width" being measured in a direction normal to the local potential contours), and makes a turn in the direction of the r coordinate at $r=r_M$. The resulting reflections of the reactive flux from the boundary appears to be responsible for the near-threshold behavior of the $F+H_2$ reaction probability.

However, this does not explain why the results from the single arrangement method are more stable and in much better agreement with the exact results at higher energies. It would appear that the $\nu=5$ state of $V(R, r_M)$, which becomes open above 0.49 eV, has a role in this. Recall that away from the boundary $r=r_M$, the exit channel solution has a significant $\nu=3$ component. In the energy range 0.28–0.49 eV, the reactive flux is directed predominantly to the $\nu=4$ state of $V(R, r_M)$, which has a very different nodal structure compared to the $\nu=3$ state. The nodal pattern of the $\nu=5$ state, on the other hand, provides a much better match to the nodal structure of the exit channel wave function. A comparison of the HD vibrational energies, also presented in Table III, explains why a similar problem does not occur in the case of the $D+HD$ reaction. In this case, the vibrational components of the exit channel solution are in good agreement, in terms of energies and nodal patterns, with the bound states at the boundary $r=r_M$.

One way to minimize the reflections of reactive flux is to modify the potential near the product boundary in such a way that the abrupt "broadening" and "turning" of the potential is made smooth and continuous. This can be accomplished by smoothly extending and "bending" the potential $V(R, r_M)$ as shown in Fig. 5(b). As one would expect from the above explanation, the total reaction probabilities from this potential, shown in Fig. 5(c), are relatively free of the effects of reflected flux.

TABLE III. The asymptotic energies in the product channel of the $F+H_2$ reaction on the TSA surface, and the $D+HD$ reaction on the PK2 surface, at a cut $r'(R' = R'_N)$ and at the cut $r=r_M$, where the primes indicate the mass-weighted Jacobi coordinates of the product arrangement. Energies are in electron volts, measured from the asymptotic minimum of the reactant molecule in both cases, and the lengths are in bohrs.

ν	HF		HD	
	ϵ_n (at $R' = R'_N = 5.27$)	ϵ'_n (at $r=r_M=3.5$)	ϵ_n (at $R' = R'_N = 7.55$)	ϵ'_n (at $r=r_M=3.0$)
0	-1.1313	-1.1966	0.2474	0.2379
1	-0.6438	-0.8362	0.7035	0.5815
2	-0.1801	-0.4870	1.1356	0.9111
3	0.2583	-0.1493	1.5434	1.2265
4	0.6687	0.1763		
5	1.0453	0.4936		
6	1.3785	0.8033		

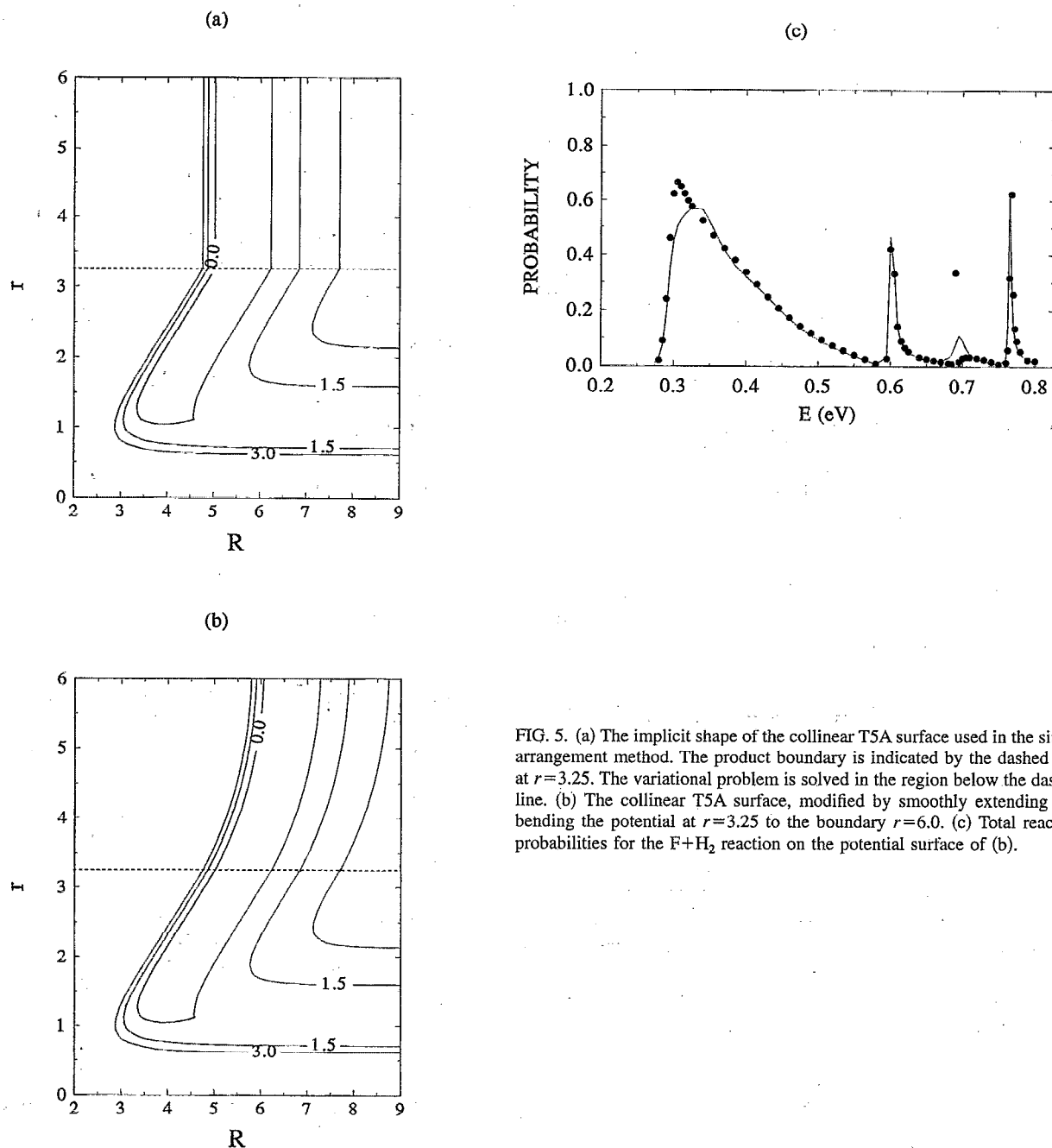


FIG. 5. (a) The implicit shape of the collinear T5A surface used in the single arrangement method. The product boundary is indicated by the dashed line at $r=3.25$. The variational problem is solved in the region below the dashed line. (b) The collinear T5A surface, modified by smoothly extending and bending the potential at $r=3.25$ to the boundary $r=6.0$. (c) Total reaction probabilities for the $F+H_2$ reaction on the potential surface of (b).

In light of these comments, it would seem that the single arrangement method has a rather limited range of applicability, unless special modifications are made to the potential surfaces. However, our experience so far indicates that the collinear $F+H_2$ is an especially severe case. In the case of 3D scattering, the product boundary typically has a much higher density of states, and the reactive flux suffers less interference from boundary reflections. In support of these comments, we present, in Fig. 6, the preliminary results of applying the method to the three 3D $F+H_2$ reaction ($J=0$) on the T5A surface *without any modifications*. Figure 6 shows that the single arrangement results are more stable as the boundary r_M is moved, and the oscillatory behavior of

the reaction probability of Fig. 4 is almost completely absent. Above $E \sim 0.285$ eV, the reactive flux appears to flow smoothly into the bound states at r_M , some of which occur at energies (in electron volts) 0.2896, 0.3135, 0.3195, 0.3644, etc. The results are also in reasonable agreement with exact results²⁷ over the energy range examined. However, since the ground energy level of the H_2 molecule at the boundary $R=R_N=6.5$ bohr is 0.2824 eV, the single arrangement method cannot reproduce the low energy "peak" in the reaction probabilities [see Fig. 2(b) of Ref. 27(b)]. Setting R_N to a larger value will yield a H_2 ground state energy less than 0.2733 eV and would presumably remedy this problem. We also expect the stability of the total reaction probabilities and

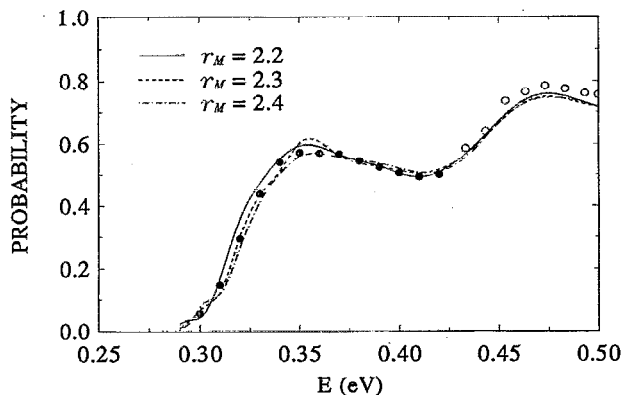


FIG. 6. Total reaction probability out of $\text{H}_2(\nu=0, j=0)$ for the 3D $\text{F}+\text{H}_2$ reaction ($J=0$) on the T5A surface. The lines represent the results of the single arrangement method at the indicated values of the parameter r_M , while the symbols are the exact results; \bullet : Ref. 27 (a) and (c), \circ : estimated from Fig. 2(a) of Ref. 27(b).

the agreement with the exact results to improve considerably if the same modification to the product channel potential as in Fig. 5 is made in the 3D case.

IV. STATE-TO-STATE REACTION PROBABILITIES

The solution of the variational problem, which yields total reaction probabilities from specific initial states under favorable conditions, also contains sufficient information regarding state-specific reaction probabilities. We now describe how this information may be extracted. Our approach is to use the open channel solutions of the variational problem to construct open channel S -matrix wave functions in each arrangement, which can then be used to directly calculate state-to-state transition probabilities.

Let n_0 denote the number of open reactant channels at scattering energy E . We number the channels such that $i \leq n_0$ denotes an open reactant state, while $i > n_0$ denotes an open product state. Then the solutions of the variational problem satisfy the boundary conditions

$$\Psi_Y^i(R_N, r) = \phi^i(r), \quad \Psi_Y^i(R, r_M) = 0, \quad \text{for } i \leq n_0, \quad (14a)$$

$$\Psi_Y^i(R_N, r) = 0, \quad \Psi_Y^i(R, r_M) = \varphi^i(R), \quad \text{for } i > n_0, \quad (14b)$$

where the superscript denotes the initial state, and the subscript on $\Psi(R, r)$ is indicative of the type of boundary conditions satisfied by the wave function. The S -matrix wave functions for the reactant initial states, on the other hand, satisfy the boundary conditions

$$\Psi_S^i(R_N, r) = h^{(2)}(k_i R_N) \phi^i(r) - \sum_{j \leq n_0} S_{ij}^Y h^{(1)} \times (k_j R_N) \phi^j(r), \quad (15a)$$

$$\Psi_S^i(R, r_M) = - \sum_{j > n_0} S_{ij}^Y h^{(1)}(k_j r_M) \varphi^j(R), \quad (15b)$$

where $h^{(1)}$ and $h^{(2)}$ are the Riccati-Hankel functions described by Calogaro,²⁸ whose asymptotic behaviors are given by

$$\lim_{x \rightarrow \infty} h^{(1)}(k_j x) = k_j^{-1/2} \exp(ik_j x),$$

$$\lim_{x \rightarrow \infty} h^{(2)}(k_j x) = k_j^{-1/2} \exp(-ik_j x).$$

The wave vectors k_j are defined with respect to the bound state energies of Eqs. (4), and the superscript on the S -matrix elements in Eqs. (15) serves to indicate that we are referring to the approximate S matrix calculated from the present method.

The first step in our procedure is to use the solutions of the variational problem to construct a set of functions satisfying the boundary conditions of Eqs. (15) as follows:

$$\begin{aligned} \Psi_S^i(R, r) = & h^{(2)}(k_i R_N) \Psi_Y^i(R, r) - \sum_{j \leq n_0} S_{ij}^Y h^{(1)} \\ & \times (k_j R_N) \Psi_Y^j(R, r) - \sum_{j > n_0} S_{ij}^Y h^{(1)}(k_j r_M) \Psi_Y^j(R, r). \end{aligned} \quad (16)$$

Consider now the mass-weighted Jacobi coordinates of the product arrangement, which we denote as (R', r') . The next step in our procedure is to identify a point R'_N along R' , and to calculate a set of product diatomic functions at this point, which satisfy

$$\left[\frac{-\hbar^2}{2\mu} \frac{\partial^2}{\partial r'^2} + V(R'_N, r') \right] \xi^n(r') = \epsilon_n \xi^n(r'), \quad n=1, 2, \dots \quad (17)$$

The choice of the point R'_N must be made such that the potential $V(R'_N, r')$ used to solve the bound state problem of Eq. (17) is sufficiently away from the "strong interaction region" that the diatomic energies are close to their asymptotic values, and at the same time, lie within the rectangular region of Fig. 1, which is spanned by the functions defined in Eq. (16). We have used the first point below the energy cut-off on the repulsive side of $V(R, r_M)$ to define the point R'_N .

Our method for extracting state-to-state probabilities now depends on the validity of the following two assumptions: (i) along the cut (R'_N, r') of the potential, the S -matrix wave functions computed using Eq. (16) are sufficiently close to the actual S -matrix wave functions; and (ii) the cut (R'_N, r') is sufficiently far from the strong interaction region of the potential that the actual S -matrix wave function can be expressed in its asymptotic form. The latter condition can be met with any desired accuracy by redefining the rectangular region of Fig. 1. We expect the former condition to be satisfied with sufficient accuracy for a large class of problems for the following reasons: we have verified that except very near the boundary $r=r_M$, the nodal structure of the scattering wave function in the r' direction is largely determined by the local potential, and also that the distortion in the nodal patterns due to the unphysical product boundary conditions applied at $r=r_M$ is significant only very close to this boundary.

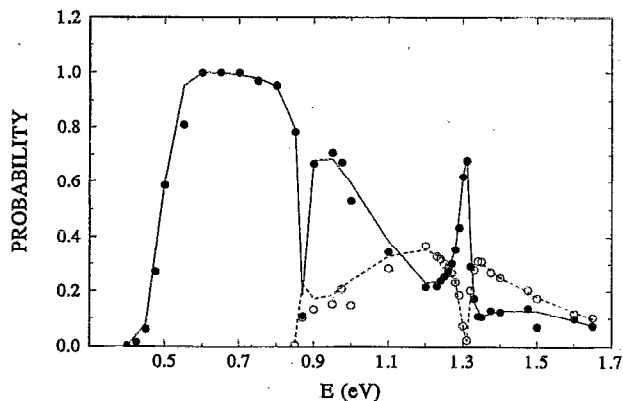


FIG. 7. State-resolved reaction probabilities using Eq. (19) (shown as symbols) compared to the exact results (lines) for the collinear H+H₂ reaction on the PK2 surface. (Solid line and filled circles) P_{0-0} ; (dashed line and empty circles) P_{1-0} .

The mass-weighted angle between the coordinate systems of the reactant and product arrangements in all the applications considered here is small enough to ensure that the range of r' (at $R' = R'_N$) for which the wave function has significant amplitude is far from the boundary $r = r_M$. In cases where the angle is too large for this to be true (e.g., Li+FH), we expect the elements of S^Y to be sufficiently close to the actual S matrix that one may extract state-to-state probabilities directly from S^Y .

Thus, in light of the above discussion, we write

$$\Psi_S^i(R'_N, r') \cong - \sum_{j > n_0} S_{ij} h^{(1)}(\kappa_j R'_N) \zeta^j(r'); \quad i \leq n_0, \quad (18)$$

where the κ_j 's are defined using the bound state energies calculated in Eq. (17). Now, taking into account the orthonormality properties of the $\zeta^j(r')$, we obtain the state-to-state reaction probability from the initial state i to an arbitrary product state k as

$$P_{ki} = |S_{ki}|^2 = |\langle \zeta^k(r') | \Psi_S^i(R'_N, r') \rangle|^2. \quad (19)$$

The state-to-state probabilities obtained using Eq. (19) for the collinear H+H₂ reaction are shown in Fig. 7 along with the exact probabilities. This comparison indicates that the assumptions made in obtaining Eq. (19) are largely justified in this case. The projections yield reaction probabilities that are qualitatively and often quantitatively in good agreement with the exact results. An extreme test of the present approach is presented in Fig. 8, where we apply Eq. (19) to the F+H₂ reaction to extract the 0-3 and 0-4 reaction probabilities, i.e., P_{3-0} and P_{4-0} . It is clear from Table III that the bound states up to $\nu=4$ at $r=r_M$ [solutions of Eq. (4b)] are open to $\Psi_S(R, r)$ just above the threshold energy. The $\nu=5$ state also becomes open at energies above 0.50 eV. The sharp mass-weighted angle between the Jacobi coordinates in this case can also be expected to cause severe distortions to the nodal patterns of $\Psi_S(R, r)$ [or $\Psi_Y(R, r)$] near $r=r_M$. In spite of this, however, Fig. 8 shows that for the range of energies where the present method yields satisfactory total

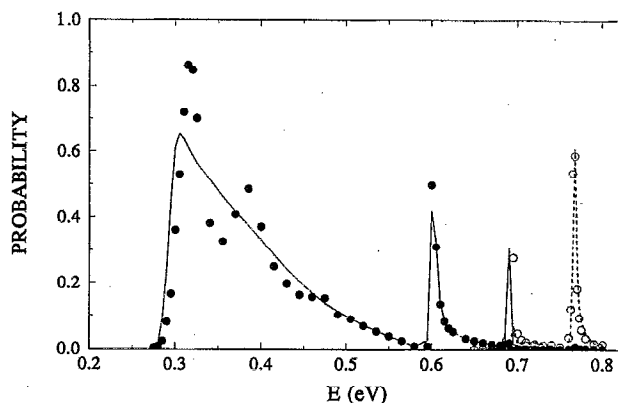


FIG. 8. The same as Fig. 7, but for the collinear F+H₂ reaction on the T5A surface. (Solid line and filled circles) P_{3-0} ; (dashed line and empty circles) P_{4-0} .

reaction probabilities, the projections of Eq. (19) also yield accurate state-to-state probabilities. However, the method has difficulty with the very narrow resonance at $E=0.690$ eV. The exact result indicates that this is a 0-3 transition, while the projection assigns the higher reaction probability to P_{40} .

V. SUMMARY

This paper presents a detailed discussion of an approximate method that reduces the formally three arrangement problem of $A+BC$ (and the two arrangement problem of collinear $A+BC$) reactive scattering to a two-point boundary value problem in a small region that spans just the reactant arrangement. The Kohn variational method for the log-derivative matrix⁹⁻¹¹ is used to solve this problem, using a Gauss-Lobatto DVR. In its present form, the region spanned by the basis has a rectangular shape, and the product boundary conditions are applied in the same direction as \mathbf{r} , the mass-weighted Jacobi vector that measures the interatomic distance in the reactant diatomic molecule. This aspect makes the method an approximate one, since the solutions in the rectangular region are matched at the 'product' boundary to functions that do not correspond to the asymptotic solutions of an actual product arrangement Hamiltonian. In spite of this, the examples presented above show that the method is capable of calculating qualitatively, and often quantitatively correct total, as well as state-resolved, reaction probabilities from a specific reactant initial state for a large class of reactions. In the case of the collinear F+H₂ reaction, for which the method yields unsatisfactory results, fairly straightforward and easily implemented modifications to the potential appear to eliminate most of the errors.

The method presented here shares many features of the approach taken by Miller and co-workers.⁵⁻⁷ The scattering problem is reduced to a linear algebraic problem. The use of the DVR renders matrix element evaluation a trivial exercise, and as shown in Tables I and II, application of the energy cut-off criterion results in substantial reductions in the size of

the basis set. Moreover, the matrices resulting from using this basis in the variational functional are extremely sparse and have a well-defined structure.

The main advantages to be claimed for the method presented here are the following: By reducing the scattering problem to a boundary value problem, we have the option of dividing the relevant region of the potential into several smaller subregions and obtaining a solution in each of them separately. For example, in Fig. 5(b), the solutions above and below the dashed line can be obtained separately and combined to yield a log-derivative matrix that connects the reactant boundary to the final product boundary. This would be the best way to extend the boundary R_N to the true asymptotic region of the T5A potential in the 3D F+H₂ reaction (see the last paragraph of Sec. III). Since smaller basis sets are sufficient to span the subregions, the individual linear algebraic problems to be solved are also smaller. Moreover, by avoiding negative imaginary potentials altogether, the present approach also avoids complex algebra in the most difficult parts of the calculations.

However, in contrast to the approach taken by Miller and co-workers, the present method incorporates unphysical boundary conditions, and computes the full scattering matrix before total reaction probabilities can be extracted. The unphysical nature of the product boundary conditions, however, can be almost completely rectified. For example, the idea of smoothly bending the potential, presented in Fig. 5(b), suggests other schemes for potential modification as well. Swinging the potential cut $V(R'_N, r')$ [see Eq. (17)] through a circular arc to the boundary $r=r_M$ would completely solve the problem of energy mismatch between components of the scattering wave function in the exit channel and at the boundary r_M . Since the exit channel is "turned" in a smooth, continuous manner, there should be minimal reflections of the reactive flux. The direction of the exit channel at $r=r_M$ would now be perpendicular to the boundary, and thus the boundary conditions applied would now be exact. Efforts to incorporate this modification, as well as to use an efficient DVR²⁹ to span the angle variable, are in progress.

ACKNOWLEDGMENTS

We gratefully acknowledge grants of CPU time on the Cray Y-MP 8/864 computer of the University of Texas Center for High Performance Computing. Financial support from the National Science Foundation and the Robert A. Welch Foundation are also gratefully acknowledged.

- ¹ X. Wu, B. Ramachandran, and R. E. Wyatt, *Chem. Phys. Lett.* **214**, 118 (1993).
- ² D. Neuhauser, M. Baer, and D. J. Kouri, *J. Chem. Phys.* **90**, 4351 (1989); D. Neuhauser, R. S. Judson, and D. J. Kouri, *Chem. Phys.* **93**, 312 (1990); *Chem. Phys. Lett.* **169**, 372 (1990); D. Neuhauser, R. S. Judson, M. Baer, R. L. Jaffe, and D. J. Kouri, *ibid.* **176**, 546 (1991).
- ³ D. Neuhauser and M. Baer, *J. Chem. Phys.* **92**, 3419 (1990); **94**, 185 (1991).
- ⁴ D. Neuhauser, M. Baer, and D. J. Kouri, *J. Chem. Phys.* **93**, 2499 (1990); D. Neuhauser, *ibid.* **93**, 7836 (1990); M. Baer, D. Neuhauser, and Y. Oreg,

- J. Chem. Phys. Faraday Trans.* **86**, 1721 (1990); I. Last, D. Neuhauser, and M. Baer, *J. Chem. Phys.* **96**, 2017 (1990).
- ⁵ T. Siedeman and W. H. Miller, *J. Chem. Phys.* **96**, 4412 (1996); **97**, 2499 (1992); W. H. Thompson and W. H. Miller, *Chem. Phys. Lett.* **206**, 123 (1993); P. Saalfrank and W. H. Miller, *ibid.* **98**, 9040 (1993).
- ⁶ W. H. Miller, *Acc. Chem. Res.* **26**, 174 (1993).
- ⁷ (a) S. M. Auerbach and W. H. Miller, *J. Chem. Phys.* **98**, 6917 (1993); (b) **100**, 1103 (1994).
- ⁸ V. A. Mandelstam and H. S. Taylor, *J. Chem. Phys.* **99**, 222 (1993).
- ⁹ D. E. Manolopoulos and R. E. Wyatt, *Chem. Phys. Lett.* **152**, 23 (1988); **159**, 123 (1989).
- ¹⁰ D. E. Manolopoulos, M. D'Mello, and R. E. Wyatt, *J. Chem. Phys.* **91**, 6096 (1989).
- ¹¹ D. E. Manolopoulos, M. D'Mello, and R. E. Wyatt, *J. Chem. Phys.* **93**, 403 (1990); M. D'Mello, D. E. Manolopoulos, and R. E. Wyatt, *Chem. Phys. Lett.* **168**, 113 (1990); *J. Chem. Phys.* **94**, 5985 (1991).
- ¹² B. R. Johnson, *J. Comput. Phys.* **13**, 445 (1973).
- ¹³ M. H. Alexander, *J. Chem. Phys.* **81**, 4510 (1984); D. E. Manolopoulos, *ibid.* **85**, 6425 (1986); M. H. Alexander and D. E. Manolopoulos, *ibid.* **86**, 2044 (1987); D. E. Manolopoulos, Ph.D. thesis, University of Cambridge, Cambridge, England, 1988.
- ¹⁴ F. Mrugala and D. Secrest, *J. Chem. Phys.* **78**, 5954 (1983); 5960 (1983); F. Mrugala, *ibid.* **91**, 874 (1989).
- ¹⁵ D. J. Zvijac and J. C. Light, *Chem. Phys.* **12**, 237 (1976); J. C. Light and R. B. Walker, *J. Chem. Phys.* **65**, 4272 (1976); D. W. Schwenke, D. G. Truhlar, and D. J. Kouri, *ibid.* **86**, 2772 (1987).
- ¹⁶ For example, see J. Z. H. Zhang, D. J. Kouri, K. Haug, D. W. Schwenke, Y. Shima, and D. G. Truhlar, *J. Chem. Phys.* **88**, 2492 (1988).
- ¹⁷ Note that the quadrature nodes are numbered $0 \cdots N$ and $0 \cdots M$, respectively. The functions u_0 and v_0 are then removed from the basis to enforce the proper boundary conditions at the origin.
- ¹⁸ In actual computations, we chose a set of "normalized" Lobatto polynomials for the basis, so that, e.g., $\langle u_i | u_j \rangle = \delta_{ij}$ when the integration is done over the quadrature grid. Normalizing the functions in this sense simply means we take the i th basis function to be $w_i^{-1/2} u_i(R)$, where w_i is the Gauss-Lobatto quadrature weight corresponding to the i th node.
- ¹⁹ J. V. Lill, G. A. Parker, and J. C. Light, *Chem. Phys. Lett.* **89**, 483 (1983); J. C. Light, I. P. Hamilton, and J. V. Lill, *J. Chem. Phys.* **82**, 1400 (1985); Z. Bacic and J. C. Light, *ibid.* **85**, 4594 (1986); **86**, 3065 (1987); R. M. Whitnell and J. C. Light, *ibid.* **90**, 1774 (1989); S. E. Choi and J. C. Light, *ibid.* **92**, 2129 (1990); J. T. Muckerman, *Chem. Phys. Lett.* **173**, 200 (1990).
- ²⁰ Y. Saad and M. H. Schultz, *SIAM J. Num. Anal.* **7**, 856 (1986).
- ²¹ M. D'Mello, C. Duneczky, and R. E. Wyatt, *Chem. Phys. Lett.* **148**, 169 (1988); C. Duneczky, R. E. Wyatt, D. Chatfield, K. Haug, D. W. Schwenke, D. G. Truhlar, Y. Sun, and D. J. Kouri, *Comput. Phys. Commun.* **53**, 357 (1989).
- ²² W. Yang and W. H. Miller, *J. Chem. Phys.* **91**, 3504 (1989).
- ²³ D. E. Manolopoulos, R. E. Wyatt, and D. C. Clary, *J. Chem. Soc. Faraday Trans.* **86**, 1641 (1990).
- ²⁴ B. I. Schneider and L. A. Collins, *Comput. Phys. Commun.* **53**, 381 (1989).
- ²⁵ B. Ramachandran, X. Wu, and R. E. Wyatt, in *Toward Teraflop Computing and New Grand Challenge Applications (Proceedings of the Mardi Gras '94 Conference, Baton Rouge, 1994)*, edited by R. Kalia and P. Vashishta (in press).
- ²⁶ R. Steckler, D. G. Truhlar, B. C. Garrett, N. C. Blais, and R. B. Walker, *J. Chem. Phys.* **81**, 5700, (1984); F. B. Brown, R. Steckler, D. W. Schwenke, D. G. Truhlar, and B. C. Garrett, *ibid.* **82**, 188 (1985); R. Steckler, D. G. Truhlar, and B. C. Garrett, *ibid.* **82**, 5499 (1985).
- ²⁷ (a) C. Yu, D. J. Kouri, M. Zhao, D. G. Truhlar, and D. W. Schwenke, *Chem. Phys. Lett.* **157**, 491 (1989); (b) Z. Bacic, J. D. Kress, G. A. Parker, and R. T. Pack, *J. Chem. Phys.* **92**, 2344 (1990); (c) D. E. Manolopoulos, M. D'Mello, and R. E. Wyatt, *ibid.* **93**, 403 (1990).
- ²⁸ F. Calogero, *The Variable Phase Approach to Potential Scattering* (Academic, New York, 1967), Appendix I.
- ²⁹ D. T. Colbert and W. H. Miller, *J. Chem. Phys.* **96**, 1982 (1992); see also Ref. 7(b); F. J. Lin and J. T. Muckerman, *Comput. Phys. Comm.* **63**, 538 (1991); Y. Guan and J. T. Muckerman, *J. Phys. Chem.* **95**, 8293 (1990).

The Journal of Chemical Physics is copyrighted by the American Institute of Physics (AIP). Redistribution of journal material is subject to the AIP online journal license and/or AIP copyright. For more information, see <http://ojps.aip.org/jcpo/jcpcr/jsp>
Copyright of Journal of Chemical Physics is the property of American Institute of Physics and its content may not be copied or emailed to multiple sites or posted to a listserv without the copyright holder's express written permission. However, users may print, download, or email articles for individual use.

The Journal of Chemical Physics is copyrighted by the American Institute of Physics (AIP). Redistribution of journal material is subject to the AIP online journal license and/or AIP copyright. For more information, see <http://ojps.aip.org/jcpo/jcpcr/jsp>